Journal of Water Resource and Protection, **2013, 5, 377-394**
http://dx.doi.org/10.4236/jwarp.2013.54038 Published Online April 2013 (http://www.scirp.org/journal/jwarp)

Laboratory Validation of an Integrated Surface Water—Groundwater Model

T. D. Sparks, B. N. Bockelmann-Evans, R. A. Falconer
Hydro-Environmental Research Centre, Cardiff School of Engineering, Cardiff University, Cardiff, UK
Email: Bockelmann-Evans@cf.ac.uk, FalconerRA@cf.ac.uk

Received November 29, 2012; revised January 5, 2013; accepted January 20, 2013

ABSTRACT

The hydrodynamic surface water model DIVAST has been extended to include horizontally adjacent groundwater flows. This extended model is known as DIVAST-SG (Depth Integrated Velocities and Solute Transport with Surface Water and Groundwater). After development and analytical verification the model was tested against a novel laboratory set-up using open cell foam (60 pores per inch—ppi) as an idealised porous media representing a riverbank. The Hyder Hydraulics Laboratory at Cardiff University has a large tidal basin that was adapted to simulate a surface water—groundwater scenario using this foam, and used to validate the DIVAST-SG model. The properties of the laboratory set-up were measured and values were determined for hydraulic conductivity (permeability) and porosity, evaluated as 0.002 m/s and 75% respectively. Lessons learnt in this initial experimentation were used to modify the flume construction and improve the experimental procedure, with further experimentation being undertaken of both water level variations and tracer movement. Valuable data have been obtained from the laboratory experiments, allowing the validity of the numerical model to be assessed. Modifications to the input file to include representations of the joints between the foam blocks allowed a good fit between the observed and modelled water levels. Encouraging correlation was observed in tracer experiments using Rhodamine-WT dye between the observed exit points of the tracer from the foam, and the modelled exit points with time.

Keywords: Integrated Surface Water Groundwater Modelling; Laboratory Experiments; Open Cell Foam

1. Introduction

Surface water and groundwater—two different resources—require careful management and protection. Computer modelling of both resources has long been used as an aid to the management of water resources. Historically, groundwater and surface water flows have been modelled separately, as their behaviour is represented by different mathematical equations and over very different time scales. However, these flow processes are a linked resource; one depends upon and impacts on the other. Groundwater provides a third of the United Kingdom's drinking water, and in some areas of southern England up to 80% of the drinking water comes from groundwater resources. Usually it requires little or no treatment before it is drinkable. However, if contaminated, these resources are expensive and difficult to restore, so groundwater needs to be protected. Surface water in rivers, lakes, estuaries and coastal systems is more visibly abundant, but no less important—its behaviour affects our everyday lives through flooding, leisure activities, transport, drinking water etc. These two resources are integral; the baseflow in streams and rivers comes from the contributing groundwater; agricultural chemicals may seep into groundwater, which subsequently may flow into streams. Accurate modelling of surface water flows needs to include contributions from groundwater resources, which can contribute significantly to the behaviour of free surface flows.

Historically, both open channel and groundwater flows have been considered for solution by numerical methods. Where the two "zones" meet, the problem has usually been approached by calculating the response of the groundwater system to changes in the river elevation [1,2]. [3] developed a model describing infiltration and overland flow based on the soil moisture properties. [4] took this approach a stage further and described numerical solutions to the coupled boundary problems representing 3-D, transient, saturated-unsaturated subsurface flow, and 1-D, gradually varied, unsteady channel flow.

A large majority of non-commercial models focus on adding surface water modules to an existing code, usually MODFLOW [5]. Most of these surface water additions are 1-D channel flow models (e.g. DAFLOWMOD-FLOW, [6]), or simple representations of larger surface water bodies (e.g. LAK3, [7]) of lake-aquifer interactions, with the exception of the wetland module [8]. This model allows 2-D overland flow through vegetation by modelling it as a porous media with a high porosity—essentially with the top layer of MODFLOW being set to high porosity and treated as a vegetated surface water. However, the channel flow is 1-D again. MODHMS [9] is the only non-commercial model found to have a distinct provision for 2-D flow on the surface, but this model is very much designed for large scale modelling, and was found best suited to including smaller surface water bodies in the 1-D channel network using a depth-area relationship. Therefore, no dedicated 2-D surface water code has been adapted to include groundwater. Combinations of two models have been used, but the surface water part is almost exclusively 1-D and unsuitable for estuaries, large rivers or coastal studies. Hence, in this study, a well-documented 2-D surface water model (DIVAST—**D**epth **I**ntegrated **V**elocities **A**nd **S**olute **T**ransport) has been extended to include 2-D and pseudo 3-D groundwater interactions within the same model, allowing smooth transition between the two areas without the common coupling problems.

DIVAST is a two-dimensional hydrodynamic and water quality numerical model, which has been developed for estuarine and coastal modelling [10-12]. The original model simulates two-dimensional distributions of surface water currents, elevations and various water quality parameters as functions of time, thereby enabling the prediction and simulation of such water management issues as pollution and flooding in surface waters. This model was extended to allow for the modelling of groundwater, as well as surface water, in the same model and thereby enabling the simulation of interactions between surface water and groundwater in the 2-D plane, in addition to the facilities of the original code [13]. The various flow interactions have been integrated within one model, by switching between the shallow water equations and the porous media equations as necessary [14,15]. The equations of flow in porous media (*i.e*. conservation of mass and Darcy's Law) have been discretised in a similar manner as the two principles on which the original DIVAST model has been based (*i.e*. conservation of mass and momentum). With the equations solved being identical to the surface-water equations in terms of the variables involved, then the difference lay in the explicit coefficients for each variable. "Groundwater" coefficients and 'surface water' coefficients were therefore defined and used according to the status of each cell, solving them together [13,16]. Extending the surface water model to include groundwater allowed water in the ground to flow over into the river—or vice versa—and for the flow to be modelled simultaneously. This approach is more suited to the "integrated river basin management" approach stipulated in the EU Water Framework Directive [17], which requires that rivers are now managed as a whole river basin, rather than artificially dividing them up into sub-watersheds or territorial boundaries.

A large tidal basin in the Hyder Hydraulics Laboratory at Cardiff University was set-up to simulate a surface water—groundwater scenario, and used to validate the refined integrated surface water/ground water model, DIVAST-SG. River banks were included in the form of permeable 60 ppi foam, which allowed a large area of groundwater to be simulated without a reinforced flume (necessary when large masses of sand are used instead). This novel approach of using foam meant that it was relatively easy to work with, and retained its shape for strong flows [13], unlike the case for sand embankments. The flume was constructed and initial experiments carried out, which included measurements of the characteristic properties of the laboratory set-up. Problems with the design and initial construction of the flume meant that only limited conclusions could be drawn from these experiments. Lessons learnt in these initial experiments were used to modify the flume construction and improve the experimental procedure, such that further experimentation was carried out on both water levels and tracer movement.

2. Flume Design and Construction

The tidal basin used in this study is a rectangular tank with a suspended floor. Before the start of this study, the water was supplied from pipes connected to the main recirculation tank. Water enters the basin through a large perforated pipe seen in **Figure 1**, and accumulates underneath the suspended base of the model. Holes in the suspended floor of the basin allowed the water level to rise to a predefined point within the flume. The water level in the main area of the flume is controlled by a movable weir on the right hand side of the figure. Water is pumped into the area between the baffle and the weir, to ensure that the water level is always the same as the weir elevation. The weir can then be raised or lowered manually or via a computer program and the water levels in the flume follow the movement of the weir. The first baffle after the weir prevents turbulence from the pumped water from entering the flume area, thus ensuring that water levels in the flume area change smoothly.

It was proposed that foam blocks were used to construct a "river-bank", and allow water and tracer to move through the idealised groundwater. Several samples of foam were obtained and tests performed to determine the approximate permeability and porosity.

Figure 1. Tidal basin at hydraulics laboratory, cardiff university. Movable weir on left, perforated inflow pipe, and baffle screen.

The foam was provided as $3\,\text{m} \times 2\,\text{m} \times 0.5\,\text{m}$ blocks. These were cut in half and trimmed using an adapted band saw to give $1.5\,\text{m} \times 2\,\text{m} \times 0.3\,\text{m}$ blocks, and several smaller blocks. Initially, the blocks were simply placed into the flume in the arrangement shown in **Figure 2**. Monitoring holes were drilled in the foam using a sharpened piece of copper pipe 100 mm in diameter.

2.1. Permeability Testing

The British Standard BS 1377 [18] describes a procedure for testing the permeability (or hydraulic conductivity) of soils. However, foam is not as straightforward to test as soil, because it does not take the shape of its container, and is generally much more porous. Before the flume was constructed, an initial test was carried out on a small sample of the foam obtained from the manufacturer. Several different samples were obtained with different numbers of pores per inch (ppi), but it was envisaged that the larger pore foam (*i.e.* fewer ppi) would be too permeable. The smallest pore foam available (60 ppi) was chosen to minimise the permeability.

2.2. Constant Head Test (Pre-Construction)

Using a sample of the foam from the manufacturer, discs were cut from the foam using a borer, soaked in water and then stacked inside a measuring cylinder of approximately the same diameter as the discs. The cylinder had a hole drilled in the base to allow water to be added. The measuring cylinder was then clamped upside down. Another, larger, measuring cylinder was placed underneath to collect the water as it flowed through. Water was added to the top of the first cylinder, and maintained at a constant head by reducing or increasing the flow as necessary. When a stable constant head was achieved, the time taken to collect a known volume was recorded from that point. Various numbers of discs were used to measure different hydraulic gradients. Using the British Standard [18] formula, the coefficient of permeability was calculated as:

$$k = \left(\frac{q}{i}\right)\left(\frac{R_t}{A}\right) \tag{1}$$

where k is the coefficient of permeability (m/s), q is average rate of flow at one hydraulic gradient (m^3/s), i is the hydraulic gradient h/L, h is the difference between the head on either side of the foam (m), L is the thickness of the foam (m), R_t is a temperature correction factor for the viscosity of water, standardised to 20˚C, and A is the area of the cross-section of the sample (m^2). The results are shown in **Table 1**.

The average permeability calculated from the results was $0.026 \pm 0.002\ \text{m/s}$. By plotting the average flow against the hydraulic gradient multiplied by the area (**Figure 3**) the line of best fit that passes through zero was found—the gradient of this line is approximate to the conductivity. This method gave a value of approximately 0.0213 m/s.

2.3. *In Situ* Permeability Test (Post-Construction)

After the foam was glued into position, further tests on the permeability were carried out. The auger-hole method is a classic field test for permeability, ideally suited to testing permeability of surface aquifers. It was planned to use this method to check the permeability of the foam once in place. However, this proved impossible as the portable pump used for the test was unable to remove water from the hole fast enough—the foam was too permeable for the hole to be pumped dry. A new pumping method was devised to allow the permeability to be measured.

Water was pumped out from one of the monitoring holes at a constant rate. The pumping maintained a constant head difference between the pumped hole and the adjacent hole. The pump flow rate was measured by collecting a measured volume of water over 30 seconds. The hole depths were measured by the use of narrow glass tubes in the hole. When a reading was taken, the experimenter's thumb was placed over the end of the tube, and the tube lifted out of the hole. The water level in the tube was then quickly measured. This was repeated to verify the depth obtained.

It was assumed that the water velocity in the aquifer was essentially horizontal and uniform over the depth (Dupuit assumption, [19]), and that the well penetrated the aquifer completely. With these assumptions it can be shown that [20]:

$$Q = \frac{\pi \cdot K \cdot \left(h_b^2 - h_w^2\right)}{\ln\left(r_b / r_w\right)} \tag{2}$$

where Q is the discharge to the pumped well (m^3/s), K is the conductivity (m/s), h_w is the depth of water in the

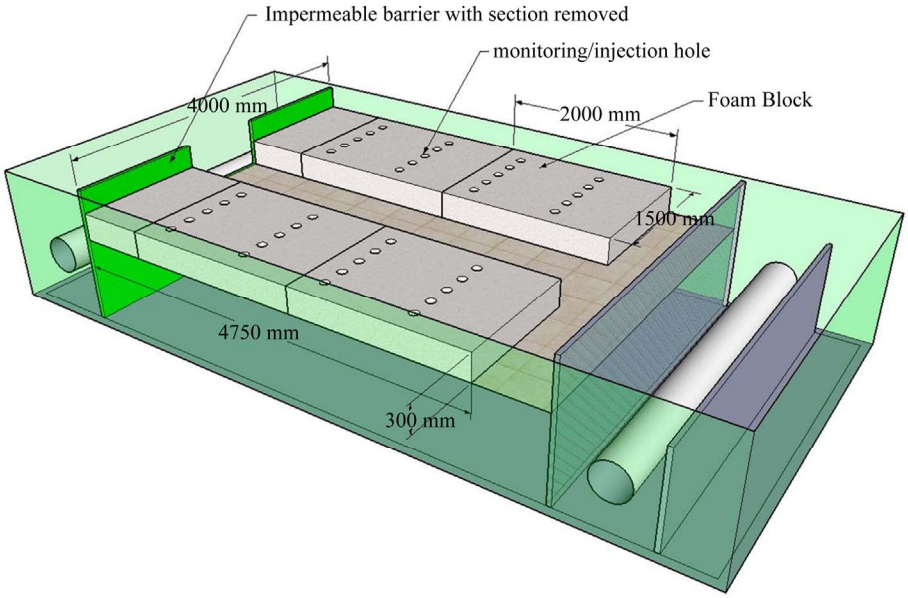

Figure 2. Layout of foam blocks in flume and initial set-up of channel.

Table 1. Summary of results and calculations.

No. of discs	*H* (head) (m)	*L* (thickness) (m)	Average flow (m^3/s)	d*h*/d*L*	Cross section area (m^2)	d*h*/d*L* *area	*K* (m/s)
2	0.033	0.030	1.29E−05	1.111852	0.0005996	0.000667	1.93E−02
3	0.033	0.045	1.02E−05	0.741235	0.0005996	0.000444	2.31E−02
4	0.033	0.060	8.44E−06	0.555926	0.0005996	0.000333	2.53E−02
5	0.033	0.075	6.02E−06	0.444741	0.0005996	0.000267	2.26E−02
					Average		2.26E−02
					Standard deviation		2.16E−03

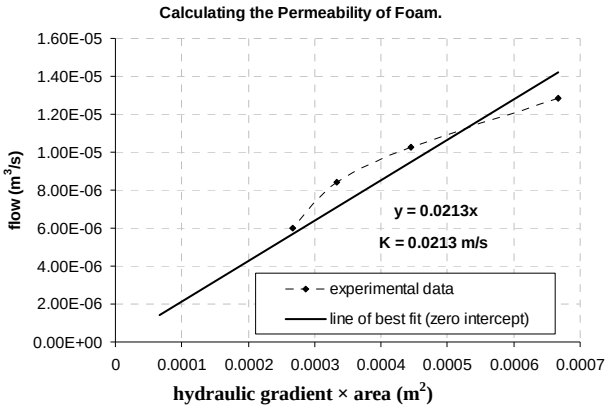

Figure 3. Hydraulic gradient × area, against flow, enabling the permeability to be calculated from the gradient of the line.

aquifer at the pumped well (m), h_b is the depth of water at the boundary well (m), r_w is the radius of pumped well (m), r_b is the radius of the circle from the centre of the pumped well to the centre of the boundary well.

Rearranging Equation (2) in terms of *K* gives:

$$K = \frac{Q \cdot \ln\left(\frac{r_b}{r_w}\right)}{\pi \cdot \left(h_b^2 - h_w^2\right)} \tag{3}$$

This equation can be used to approximate the permeability of the foam. The experimental results and calculated permeabilities are shown in **Table 2**.

This can be confirmed by an iterative method carried out as follows. A linear head distribution between the two wells was assumed to start with (with heads at the wells being taken from the data collected above), and the permeability was estimated at intervals between the two wells, using Darcy's Law (Equation (1)). If the estimate of the head distribution is correct, each interval should give a similar value for the conductivity. The initial linear head distribution gave values for *K* which vary widely between the wells, and so was obviously incorrect. The heads across the area were then varied according to an arbitrary equation based on $y = \sqrt{x}$, and iteration was halted when the variation of the *K* values across the domain was at a minimum.

Table 2. Pumping test to determine conductivity.

Pumped Well				Boundary Well							
Well No.	Measured Water Depth (m)	Plug Depth (m)	Actual Water Depth (m)	Well No.	Measured Water Depth (m)	Plug Depth (m)	Actual Water Depth (m)	Q (m^3/s)	Boundary Radius (m)	Well Radius (m)	K (m/s)
14	0.171	0.0540	0.2250	13	0.212	0.0395	0.2515	0.0004	0.5	0.025	0.0302
5	0.230	0.0255	0.2555	6	0.265	0.0290	0.2940	0.0002857	0.5	0.025	0.0129
7	0.155	0.0410	0.1960	8	0.215	0.0405	0.2555	0.000333	0.5	0.025	0.0118
16	0.153	0.0415	0.1945	15	0.213	0.0435	0.2565	0.0002857	0.5	0.025	0.0097
5	0.183	0.0255	0.2085	6	0.206	0.0290	0.2350	0.000333	0.5	0.025	0.0270
1	0.140	0.0525	0.1925	2	0.163	0.0425	0.2055	0.0001975	0.5	0.025	0.0364
										Average	0.0213

The head distribution obtained by this method was confirmed visually to be close to the expected distribution (**Figure 4**). Therefore the stable value of *K* was used as an estimate of the conductivity. Values obtained are shown in **Table 3**.

The iterative values agree closely with the equation values for conductivity, showing that the assumptions made when using the equation were valid. Also, the *in-situ* results agree well with the previous constant head experiment. It was therefore concluded that the conductivity of the foam was approximately 0.021 ± 0.01 m/s, *i.e*. it lies between 0.03 and 0.01 m/s. **Table 4** shows the values of conductivity of the foam found by the different methods.

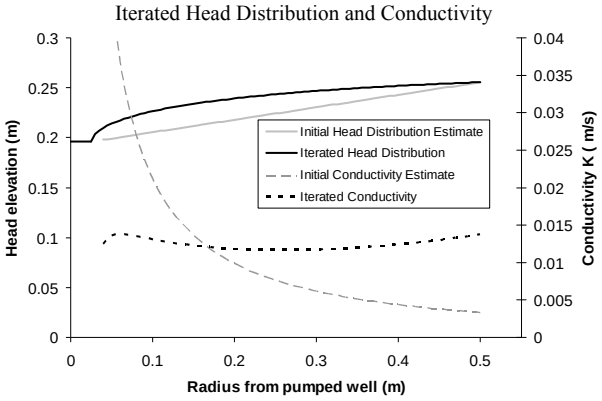

Figure 4. Example of iterative predictions of conductivity (Test number 3). Head distribution is varied until the variation in *K* (dotted line) is a minimum.

Table 3. Iterative *K* values compared to theoretical *K* values from theoretical equation.

	Iterative *K*	Theoretical *K*	Difference
Test 1	0.03276	0.03021	0.0026
Test 2	0.01359	0.01288	0.0007
Test 3	0.01233	0.01182	0.0005
Test 4	0.01015	0.00974	0.0004
Test 5	0.02858	0.02702	0.0016
Test 6	0.03870	0.03640	0.0023
Average	0.02269	0.02134	
Stdev	0.01110	0.01028	
Max	0.03870	0.03640	
Min	0.01015	0.00974	

2.4. Porosity

Porosity tests were carried out on a cylinder of foam cut from the main block, which was measured and weighed while dry. It was then completely saturated by submersion and squeezing. When no more air bubbles were produced it was quickly transferred above a measuring cylinder and allowed to drain under gravity. The amount of water drained was recorded. Then, the small portion still saturated at the base of the cylinder was gently squeezed to release the water held. The total amount drained was recorded again. Then the cylinder was squeezed completely to remove as much water as possible by hand. This final amount was also recorded. Finally, the damp cylinder was re-weighed to measure the amount of water retained in the pores. From these measurements several different porosities can be calculated (**Table 5**).

The total porosity of the foam was found to be nearly 80%, the effective porosity was estimated at approximately 75%. Therefore the foam is much more porous than an equivalent sand or soil.

3. Initial Experimental Work

This section of the study comprises experimental work that laid the groundwork for the subsequent experiments but encountered several problems which are summarised at the end of this section, along with the solutions that were proposed to solve them. The numerical modelling in this section is only sparingly referred to, because the model set-up is described in detail in later sections.

Table 4. Conductivity values for the laboratory foam.

	Average Value of K (m/s)	K (cm/s)	+ or – (Error m/s)
Constant Head Test Numerical	0.02600	2.600	0.002
Constant Head Test Graphical	0.02130	2.130	n/a
In-Situ Test Iterative	0.02269	2.269	0.011
In-Situ Test Theoretical	0.02134	2.134	0.010

Table 5. Calculating the porosity of the foam.

Cylinder of Foam Details	Measurement		Porosities	
Dimensions				
Diameter	50	mm		
Height	272	mm		
Dry Mass (A)	12.395	g		
Gravity Drained (B)	260	ml	0.486827	48.68%
Remaining Saturated Portion Squeezed Out (C)	375	ml	0.702154	70.22%
Cylinder Squeezed—As Much Water Removed as Possible (D)	400	ml	0.748964	74.90%
Final Mass of Cylinder (E)	31.41	g		
Water Remaining in Cylinder $(E-A)=(F)$	19.015	g		
Total Water Held in Foam $(D+F)$	419.015	ml	0.784568	78.46%
Volume of Cylinder $(G)=\pi\times(d/2)^2\times\text{Height}$	534.0708	cm^3		

The set-up reflected an idealised tidal river basin that could be easily modelled numerically and physically. The tide at one end was varied sinusoidally via the computer controlled weir. The concentrations of dye used in the experiment, the settings of the measuring equipment, and the amount of dye solute used in the model were predetermined with the help of the computer model. The results obtained were then corrected for delays and background concentration, and subsequently compared to the computer model output.

3.1. Initial Experiments

Rhodamine WT was used as a highly specific tracer [21], which is non-toxic, usable in small quantities, cost-effective, easy to measure at very low concentrations, and stable during the course of the study. The channel was constructed out of 60 ppi foam blocks with dimensions as shown in **Figure 5**. The foam is intended as porous media through which water and solute can flow as if through a river bank. The foam was glued to the base of the flume, but very quickly after the water was introduced the glue failed and the foam floated. In order to keep the foam attached to the base of the flume weighted

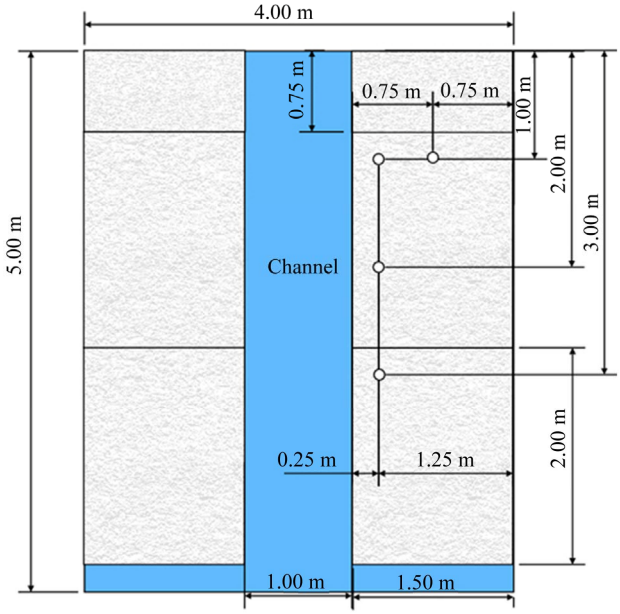

Figure 5. Flume design.

boards were used on top of the foam. Monitoring/injection points were cut out of the foam with a copper tube of 100 mm diameter. The holes went through the entire depth of the foam, and the extracted core was retained for reinsertion if needed. The position of the injection point was selected so that it was some distance from the top and side boundaries to reduce interference with contaminant accumulating by the walls. This allowed the migration of tracer along the channel and the bank to be investigated, while minimising unwanted effects of conducting the experiments in the laboratory with walls, rather than in a real river. The flume and monitoring/injection points are shown in **Figure 6**. Two monitoring points were selected both from the practical and analytical point of view to enable detection of the tracer plume. Point "A" was selected along the perpendicular line from the outfall location to the channel. Point "B" was selected to help investigate the spread of contaminant due to diffusion along the foam (see **Figures 5** and **6**).

3.2. Instruments

Two 10-AU fluorometers were calibrated and used to measure simultaneously the concentration of the dye at the two monitoring points. A peristaltic pump was used to obtain the water sample at the monitoring locations, set to a low pumping rate so as not to interfere with the flow or water levels in the flume. The travel time for flow through the pipe was measured, and the results adjusted accordingly. The sampling point was positioned at an elevation just below the lowest water surface elevation (100 mm from the floor of the flume) in order to keep it submerged even at low tide.

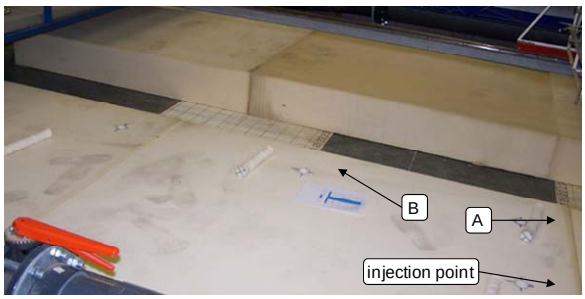

Figure 6. Flume with no water, showing location of injection and monitoring points (A + B).

3.2.1. Experiments

The flume was driven by a sinusoidal water elevation boundary, varying from 290 mm to 110 mm and back over a 30 minute period, to simulate a tidal boundary. Rhodamine WT tracer was injected at the injection point over a period of 2 minutes at a concentration of 1 g/l. The dye was injected at t = 1800 s, *i.e*. at the peak of a tidal cycle. The volumes injected were 50 ml, 75 ml and 100 ml. Initial experiments for 100 ml injections showed the concentrations were too high to measure, so subsequent experiments were performed with 75 ml and 50 ml injections.

3.2.2. Numerical Modelling

DIVAST-SG was set-up to model the physical laboratory flume using a 10 cm grid. A water elevation boundary was imposed at the lower end of the flume using a sinusoidal wave of 30 min wavelength, 0.09 m amplitude and mean water level of 0.2 m. A porosity of 0.75 and a permeability of 0.02 m/s were used.

Figure 7 shows typical data measured at monitoring point A. The data shows good correlation for the timing of the peaks between the numerical and physical models, although there are a few points that indicate that improvements are needed to be made in the physical model. These are discussed in sequence.

The predicted peaks are much higher than the measured peaks. The maximum concentration in the numerical model is 7.5×10^{-4} g/l , (or 750 ppb). The values observed are approximately an order of magnitude below this. This indicates that much of the dye has been "lost" from the foam. Some of the dye has probably been lost due to adsorption to the foam, but it seems likely that for the effect to be this large, a lot of the dye is likely to have entered the surface water via a short-circuit underneath the foam. The initial experiments conducted support this theory; these were done while the foam was still firmly attached to the base of the flume (before the buoyancy of the foam defeated the glue) and when the concentrations were measurable they were much closer to the predicted order of magnitude (*i.e*. time 9000 - 9900 s, predicted range of 250 - 300 ppb, measured range of 175 - 450 ppb).

The peak shown in **Figure 7** at about 1000 seconds occurred before the dye injection, and so is probably due to background dye from previous tests. The similar shape of the peaks from 6300 s to the end of the test may point to a similar source, rather than a gradual dispersion from the injection point. The peaks occur during the rising of the tide, when the rising water re-enters from the channel into the foam and towards the monitoring points. This suggests that after t = 7200 s most of the dye detected originated from the channel, with small amounts from the foam. It is not clear as to what extent the peaks are caused by water flowing through the foam, along the suspended floor of the basin, or rising from the larger basin underneath the suspended floor. The sharp peaks occur at a particular level of the rising tide, which could be associated with the critical amount of water necessary to cause enough buoyancy within the foam to lift it enough to allow water flow underneath. In contrast, the numerical model predicted a decrease in concentration as the tide rose, as the cleaner water from the channel entered the foam.

The flow of water within the foam is slow and facilitates tortuosity of the flow paths of particles, which aids diffusion and dispersion of the dye, causing more scattering of the particles. Therefore the shape of a peak is a significant indication of its origin. A round peak indicates that the contaminant is more scattered within the water and it is likely that this reflects dye flowing through the foam. A sharp spiked peak is more characteristic of a source where the dye remains as a well defined "slug", indicating a short-circuit from the injection point or other dye-rich area. Hence, it was regarded as likely that the rounded peaks, which occurred just after low water were from a diffuse source (*i.e*. had travelled through the foam). The timing of these rounded peaks matched up well with the predicted peaks in the numerical model. In between these peaks the concentration dropped back down almost to the background level very quickly. Again, this indicates that the monitoring holes were connected to the main channel by short-circuiting. If the dye was leaving through the foam then the concentration would reduce much more gradually.

The numerical model predicted that the concentration at point "B" would slowly increase with time as the dye diffused longitudinally through the foam, but the measured values showed no sign of this prediction, only the same increasing background peaks as seen in **Figure 7**. The dye did not reach this second monitoring point as expected; another sign of short-circuiting of the tracer.

The foam is buoyant, so in order to stop it rising, it was glued to the base of the flume. However, after the first experiment, sections of the foam had lifted away from the flume base. Weighted boards were placed across the foam, but from the results it seemed they were insufficient to

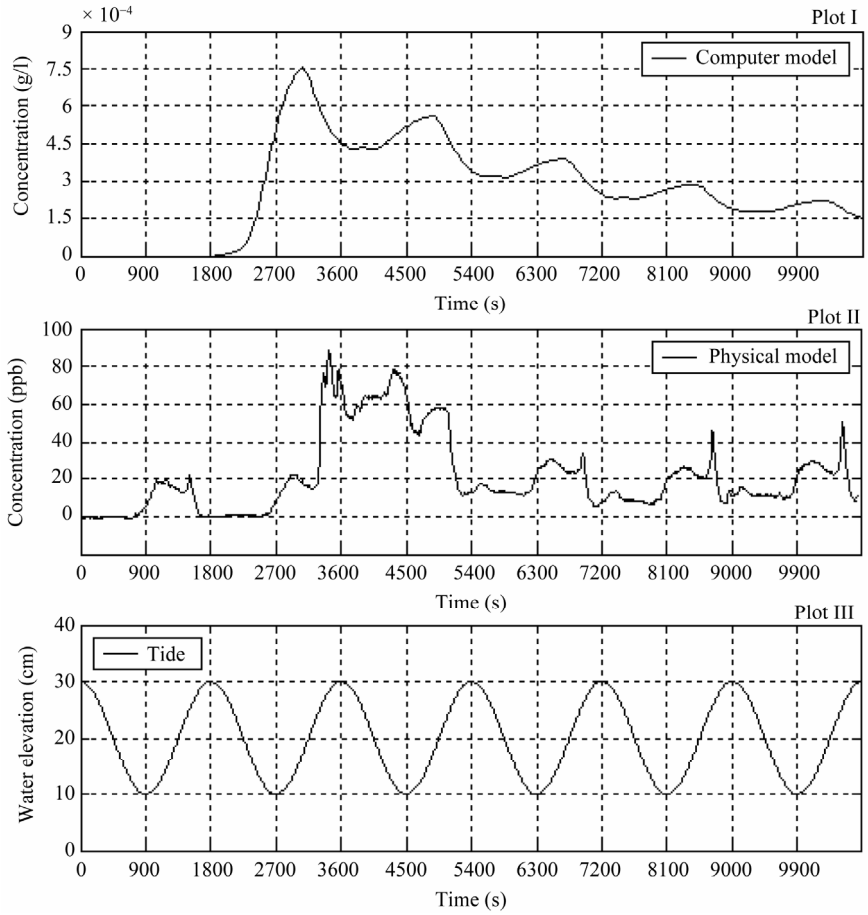

Figure 7. Plot I—Graph of the numerical prediction of change of concentration of Rhodamine WT with time at point A for 75 ml of 1 g/l dye injected over two minutes; Plot II—The concentration of Rhodamine WT recorded at point A during physical experiment 4; Plot III—The respective tidal phase.

prevent short-circuiting of the water underneath the foam.

4. Adapting the Flume

The initial experiments highlighted numerous problems with the physical setup, mostly involving short-circuiting water under the foam. In order to solve these problems the following steps were taken. A stronger water-activated glue was sourced and tested on small samples of the foam. The new glue proved to be much stronger than the previous glue used.

More monitoring holes were drilled in the same way as before. Small discs of foam were reinserted into the base of the holes and glued into place so that if the foam did lift off the bed of the flume, there would be no direct contact between the water beneath the foam and the monitoring/injection holes. The foam blocks were reattached to the bed of the flume using the water-activated glue. The foam blocks, once in the flume, were glued in strips at the joints, in an attempt to limit seepage along the cracks but still allow flow between blocks.

After the initial tracer and water level experiments proved inconclusive, the flume features were changed. The main "river" channel was blocked off with a wall at the end furthest from the weir. A section of this barrier was removed on one side to allow the upstream reservoir area to be in direct contact with the foam, and water was then pumped into this area. This created a permanent head difference between the upper reservoir and the main channel, causing a constant flow through the foam connected to the reservoir, which was missing in the previous set-up. Before, the flow in the groundwater oscillated with the tide, and as a result, the injected tracer tended to remain in the groundwater, shifting side to side with the tide. With the new set-up, injected tracer flowed from the foam into the main channel, allowing it to be measured on the way, and also when it reaches the channel.

4.1. Water Level Measurements

Water level data was collected in the monitoring holes using two wave probes. These devices consist of two parallel stainless steel wires which are immersed in the water. The electrical conductivity between the wires varies

depending how deeply the probe is immersed. Therefore, by calibrating the probes at known depths, a real-time measure of water levels can be obtained. The calibration can be checked *in-situ* by measuring with a ruler and then the wave-probes used with confidence for a number of scenarios. The monitoring holes are referred to in the scheme shown in **Figure 8**. The measured data is shown in **Table 6**. The measured data was interpolated and a contour plot produced as shown in **Figure 9**, giving a visual approximation of the measured head distribution.

4.2. Setting up the Model (Water Levels)

DIVAST-SG was set-up to simulate the laboratory flume set-up. The code was modified to allow multiple water elevation boundaries to be specified and two water elevation boundaries were set up. Monitoring points were created at the locations of the monitoring holes in the foam. Permeability was set to 0.02 m/s , and porosity to 0.75. The initial model run results are compared to the measured elevations in **Figure 10**.

It can be seen in **Figure 10** that the measured elevations are significantly lower than the modelled elevations. Because the situation is steady-state (*i.e.* the boundary conditions are not changing) the head distribution is unrelated to the permeability and porosity values. Changing

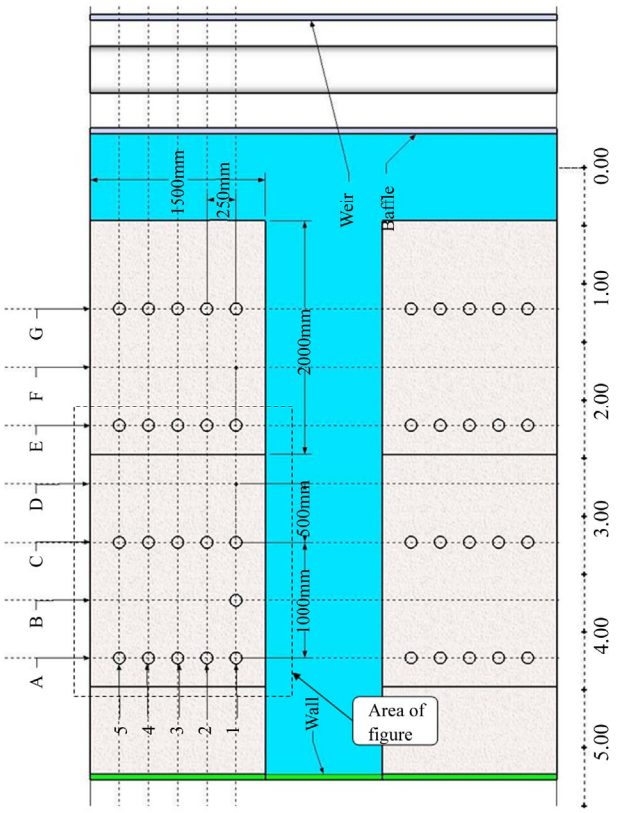

Figure 8. Schematic diagram of the tidal flume showing labelling of monitoring holes and reference ruler.

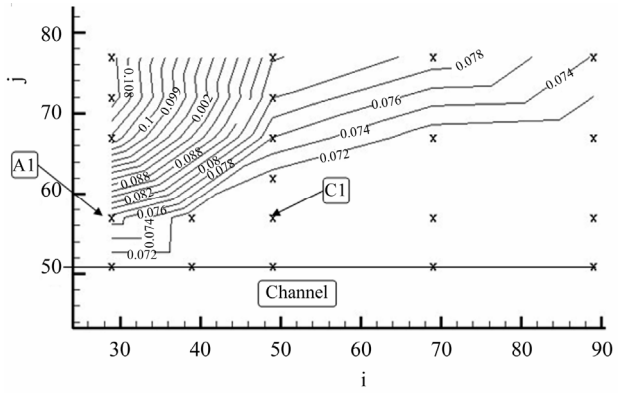

Figure 9. Interpolated contour plot of measured elevation data in the foam (*i* and *j* units are ×5 cm: the grid size used in the model).

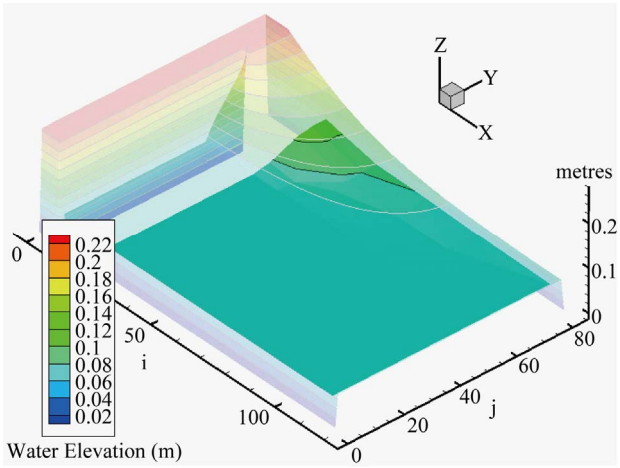

Figure 10. Measured water elevations (solid) compared to initial modelled elevations (transparent). *i* and *j* axes are in ×5 cm from edge of the model, or grid cell reference coordinates.

Table 6. Measured water elevations at steady state.

Location	Measured Water Elevation (mm above Flume Floor)	Details
Channel at A	70.00	Water Level behind Barrier
A1	77.00	227 mm
A3	103.70	
A4	109.40	Water Level in Channel
A5	108.80	70 mm
B1	70.30	
C1	70.00	
C2	71.00	
C3	76.00	
C4	80.10	
C5	82.20	
D1	70.00	
D3	70.60	
D5	79.40	
E1	70.00	
E3	70.00	
E5	73.90	
Channel at E	70.00	

these values in the model does not enable a better fit to the measured data to be obtained. Therefore, the model was not correctly simulating the head distributions in the flume, which were much lower than the model predicted.

The most likely cause of this was thought to be the structure of the laboratory foam. The blocks of foam were originally glued together in strips in an attempt to reduce the possibility of water finding preferential pathways between the separate blocks, but from the measured data, it appeared that the water was escaping along the joints between the blocks, and therefore lowering the measured elevations. To test this, the model domain was altered, and the following methods of including the joints between the foam in the model were tested: increasing permeability along the joints e.g.

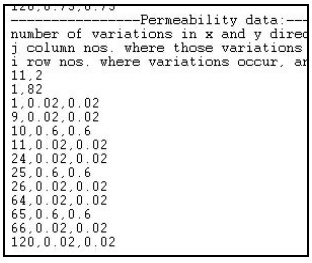

including open cells in between glued areas on the joint, e.g.

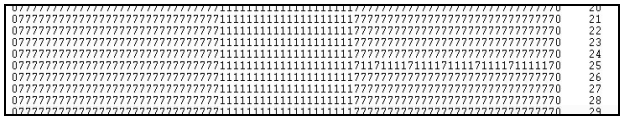

modelling the joint as all open cells separated from the channel by a few foam cells, e.g.

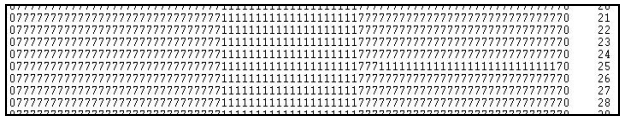

combinations of the above methods (**Table 7**). A series of methods for modelling the joints was tested (**Table 8**).

It can be seen from **Figures 11** and **12** that using a combination of the approaches gives the best results, with model run 4e being closest to the measured data in gradient and elevation. **Figure 13** shows the measured and modelled data for the same two cross-sections just for model run 4e. This model set-up used open cells at the joints for half the width of the foam and an increased permeability (0.6 m/s) for the other half (nearest the channel) of the joint.

4.3. Discussion of Water Level Experiments

Water levels in the foam were measured under several scenarios, by the use of wave probes to give continuous readings of water levels. These were periodically calibrated and confirmed by using simple ruler measurements. In the end, steady state water levels were used to check correlation between the numerical model and the physical model.

The first round of experiments highlighted problems with the use of foam as a porous medium to simulate the flow of groundwater, mostly caused by the buoyancy of the foam. Most of these problems were addressed by the use of a much stronger adhesive to attach the foam to the flume floor. However, from the new measured data it was clear that another factor was still affecting the water levels. The water level experiment described was designed to produce results independent of the permeability and porosity parameters. The water elevations were based on the steady-state boundary conditions, which are duplicated as precisely as possible in the numerical model. Yet, the measured values differed considerably from the numerical predictions, e.g. at the wall side of section A the initial modelled value was 0.177 m, but measured at 0.108 m, a difference of 7 cm or 65% of the measured value. This indicated that the initial numerical model did not duplicate the physical situation precisely.

The initial model run shows a smooth groundwater slope from the top edge of the foam to the channel. The measured data was only measured below the first joint in the foam, but showed a much lower elevation than the initial numerical model predicted. This indicated that somewhere between the top edge of the foam and cross-section A, a significant head loss was occurring in the physical model. The obvious location of this head loss was at the edge of the foam (along row i = 10 of the numerical model), and at the first joint between the foam blocks (along row i = 25 of the numerical model). The measured data at cross-section A also shows a drop in elevation towards the wall of the flume, indicating that perhaps water was seeping along the wall boundary also.

Numerous approaches of introducing this head-loss into the numerical model were tried by varying the permeability and adding surface water (open) cells. The best results were obtained when the numerical model was adjusted by increasing the permeability of the foam along the joint locations (to approximately 0.6 m/s), and in addition a number of surface water cells were included at the joint between the foam blocks (as if the joint were not glued together) on the side of the foam furthest from the channel. The fact that this scenario gave numerical results that fit the measured data suggests that the joints were indeed responsible for the head-loss in the physical model. However, the way in which these parameters for the joints was determined was somewhat arbitrary, as the permeability of the joint was impossible to determine in practice, and the joint did not open up as wide as the open cells in the nu-

Table 7. Methods of joint modeling.

Run number	Method of joint modelling
1a	Permeability of joint 0.1 m/s
1b	Permeability of joint 0.6 m/s
2	Glued joints (no permeability change)
3a	Open cells—1 cell of foam between channel and joint (no permeability change)
3b	Open cells—3 cells of foam between channel and joint (no permeability change)
4a	Glued joints (permeability 0.1 m/s)
4b	Glued joints (permeability 0.6 m/s)
4c	Open cells—3 cells of foam between channel and joint (permeability 0.1 m/s)
4d	Half open cells (permeability 0.1 m/s)
4e	Half open cells (permeability 0.6 m/s)

Table 8. Experimental data for selected tracer experiments.

Reference	Date	Pump Started at	Time Injected	Tracer Volume (ml)	Tracer Concentration (ppt)	Injection Duration (seconds)	Water Level Upstream (cm)	Water Level in Channel (cm)
Nov 2 B	02/11/2006	11:50	11:56	100	1	103.00	27.0	11.0
Nov 9 A	09/11/2006	10:10	10:31	100	1	80.00	27.5	11.2
Nov 9 B	09/11/2006	10:10	15:12	100	1	77.00	26.0	11.2
Nov 10	10/11/2006	09:50	14:59	100	1	75.00	26.0	11.9
Jan 12	02/01/2007	08:30	11:58	100	1	79.00	18.0	8.1
Jan 29	29/01/2007	10:30	18:05	100	1	79.00	24.0	8.0
Jan 31	31/01/2007	10:15	16:18	100	1	79.00	24.0	8.0
Feb 5	05/02/2007	12:00	20:36	100	1	78.00	26.0	8.0
Feb 7	07/02/2007	09:50	15:59	100	1	79.00	26.7	8.0

Ref	Logging Started at	Injection Borehole	Position of Fluorometer 1	Position of Fluorometer 2	Position Tracer Entered Channel (m on Flume Ruler)	Time Tracer Entered Channel (Minutes after Injection)
Nov 2 B	11:55	A3	C3	C1	2.82	8.00
Nov 9 A	10:29	A5	C4	C2	2.75	62.32
Nov 9 B	16:26	A5	C1	C1	2.78	56.00
Nov 10	14:58	A5	Not Used	Not Used	2.89	57.66
Jan 12	12:00	A5	Not Used	C5	Not Known	Not Known
Jan 29	18:01	A5	C3	C3	2.75	54.00
Jan 31	16:16	A5	C5	C5	2.75	54.00
Feb 5	20:34	A5	Channel at 2.5 m	Channel at 2.5 m	2.75	54.00
Feb 7	12:00	A5	Channel at 2.5 m	Channel at 2.5 m	2.75	52.50

Ref	Notes
Nov 2 B	Small amount of dye observed in channel at 12:03 at 2.82 m on side ruler Lots of dye observed emerging at about 12:07, at the 3.8 m mark More dye emerging from 2.8 m at approx 12:13, (12:15?) continues until 12:37 ish
Nov 9 A	
Nov 9 B	After time 1:18:57 the point of entry had moved to 2.69 m
Nov 10	At time 1:31 the point of entry into the channel had moved to 2.75 m. At time 1:41 the point of entry into the channel had moved to 2.65 m
Jan 12	Peak detected in C5
Jan 29	No peak detected
Jan 31	Peak detected in C5
Feb 5	Peak detected on both fluorometers
Feb 7	No peak detected, but dye observed. Fluorometer malfunction?

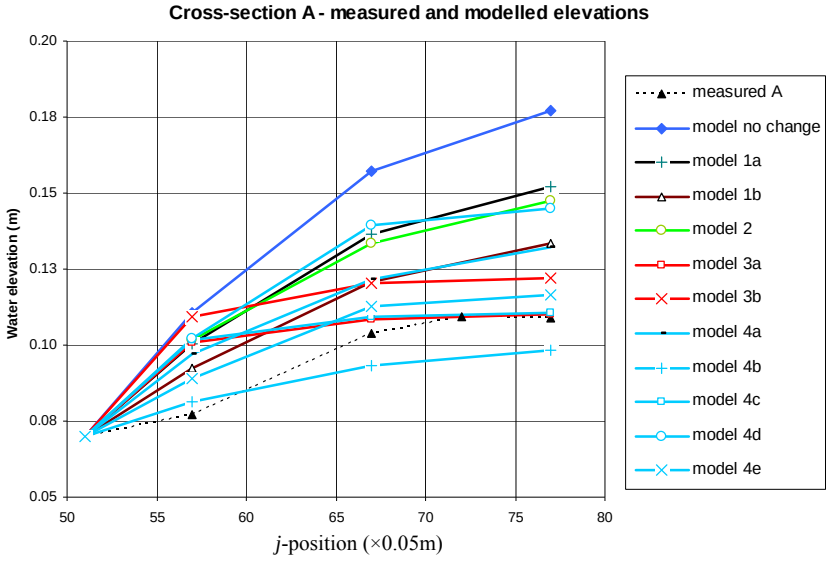

Figure 11. Measured and modelled elevations for cross-section A. *j*-position is in grid cell reference or ×0.05 m from the edge of the model.

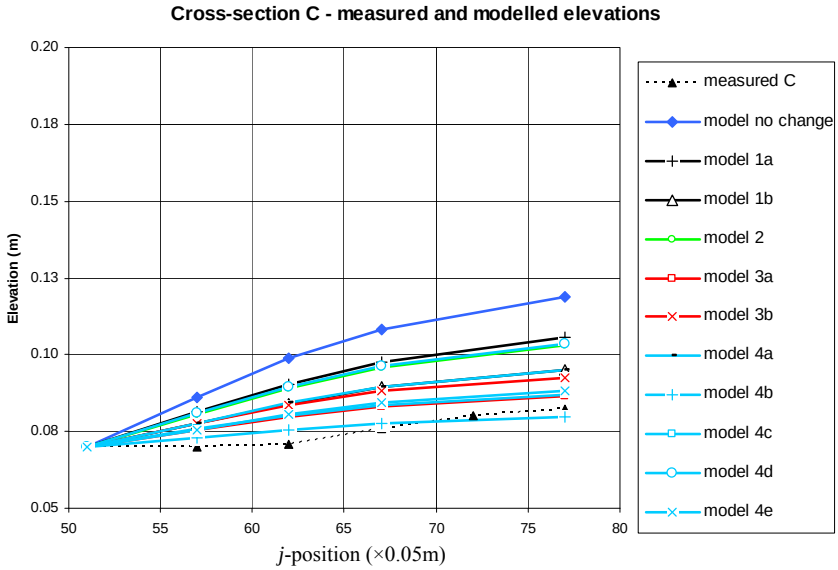

Figure 12. Measured and modelled elevations for cross-section C. *j*-position is in grid cell reference or ×0.05 m from the edge of the model.

merical model would suggest. By trialling several different approaches of modelling the joints in the model set-up, a good agreement between the measured and modelled data was obtained. For example, at hole A5, the elevation was modelled at 0.116 m, and measured at 0.108 m, only a 0.8 cm difference, 7% of the measured value, much improved from the 7 cm (65% difference) initially.

The remaining differences could be due to the fact that unsaturated flow is not included in the model. The model assumes there is no water above the water table, but in actual fact this area is variably saturated. This problem was minimised by allowing the scenario to settle in its steady state for some time, as most of the unsaturated behaviour occurs as the water level in the foam changes. However, even with the steady state set-up, the unsaturated portion of the foam could be affecting the flow behaviour. Seepage faces, where the groundwater exits above the surface water level and trickles down the face were observed along the channel face of the foam, but mainly during transient scenarios where the water level in the channel drops rapidly—during the steady state scenarios they disappear once equilibrium is reached.

In this way the water level data collected from the laboratory was used to refine the numerical model until relatively good agreement was reached. The numerical model was actually essential to understanding what proce-

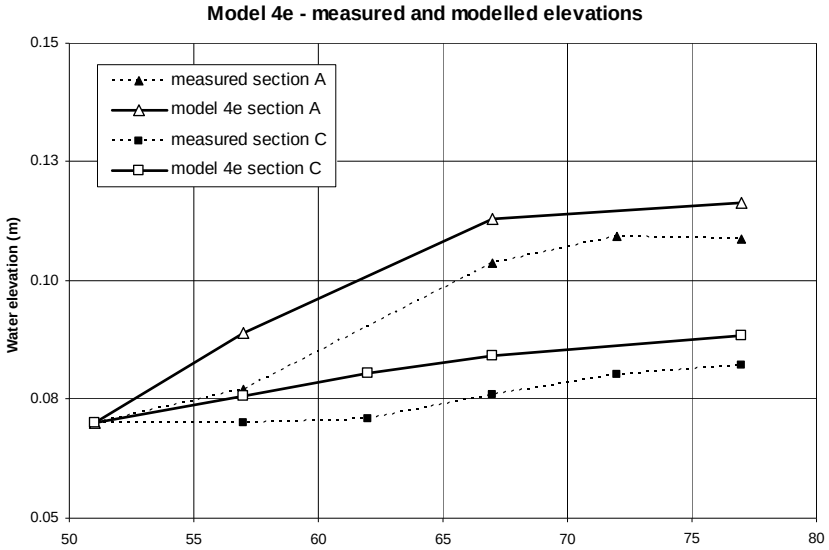

Figure 13. Measured and modelled elevations for both cross-sections and model run 4e.

sses were occurring in the physical model. By modelling increased flow rates along various joints in the foam it was concluded that preferential pathways existed in the physical model—while these were unintended in the original physical model plan, with hindsight, perhaps they were difficult to avoid—and they have served to show that the numerical model is flexible enough to include unforeseen elements such as these. The water levels in the physical model are now closely predicted by the numerical model (with a difference of the order of 5 - 10 mm), but the exact flow structure at the joints may not be correctly predicted because of the subjective nature of the adjustment to the numerical model. The adjusted numerical model can be used in the tracer experiments to assess the solute transport response.

5. Tracer Experiments

Monitoring holes in cross-section A were used to inject tracer into the foam under the same steady-state conditions described previously (**Figure 2**). The water level at the head of the flume behind the foam, and the water level in the channel were measured and recorded after steady state conditions were obtained. 100 ml of Rhodamine WT at 1 ppt was then injected into the monitoring hole using a burette over a period of approximately 1 min 30 sec, although this varied slightly for each experiment depending on the burette used. The exact injection time was recorded in each case. The two fluorometers were placed in other monitoring holes to record the concentration of dye passing through (**Figure 14**).

Each monitoring hole was measured in turn (using both fluorometers in the same hole) over approximately 2 hours to allow the dye to fully move through the foam. Before each experiment the steady state pumped head was maintained for at least an hour to ensure the dye from the previous experiment had been flushed through the foam.

When injected into hole A5, the dye consistently exited the foam around the location of cross-section D (**Figure 8**), approximately one hour after injection. Readings were taken from all holes along cross-section C, however, only in hole C5 were any significant dye concentrations recorded (**Table 7**).

5.1. Numerical Modelling of Tracer

The model that most accurately predicted the water levels in the previous section was taken and a conservative tracer (referred to as salt in the input files) was used to represent the Rhodamine WT. This tracer was added to the model at 0.35 hours to allow time for the water levels to stabilise to the desired levels. The water levels and injection location and duration were set in each input file to reflect each experimental run being modelled.

The tracer results were collected in two methods—the detailed fluorometer data from the monitoring holes, and the exit point and time of the dye emerging from the foam into the channel. Time and location of the modelled tracer plumes first visibly emerging from the foam in the laboratory were recorded (**Figure 15**). The axes are the model grid co-ordinates or ×10 cm from the edge of the flume. The tracer concentration is in ppt. All the runs have tracer injected into hole A5, except from runs Nov 2 B and Nov 2 C, where the tracer was injected into hole A3. Exit points were predicted for all the runs listed in **Table 7** with the exception of Jan 12, when no exit point was recorded. A video of the flume shows the tracer emerging from the foam after injection into A5. It can be seen that the tracer exits the foam and continues downstream, as would be expected. In the model, the tracer

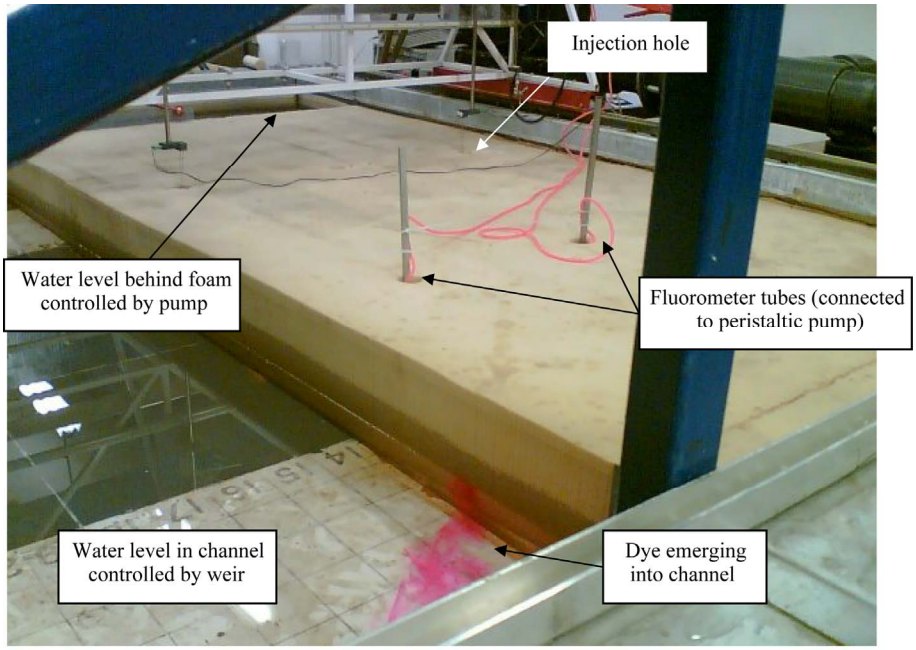

Figure 14. Tracer experiment in progress, showing injection hole, two fluorometer measuring points, wave probes in upper holes, and dye emerging into the channel.

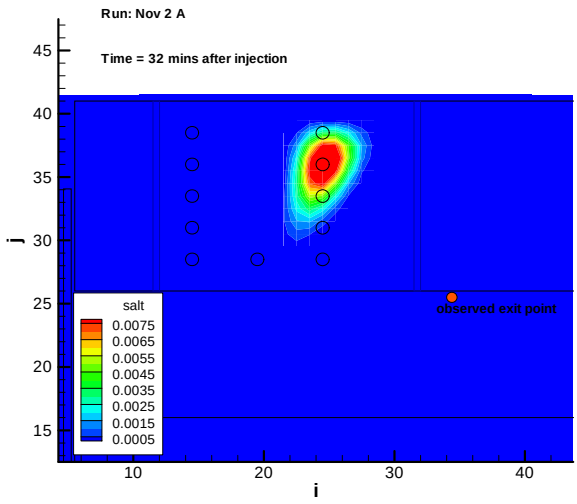

Figure 15. Observed exit point and modelled tracer plume for Nov 2 A at 32 min.

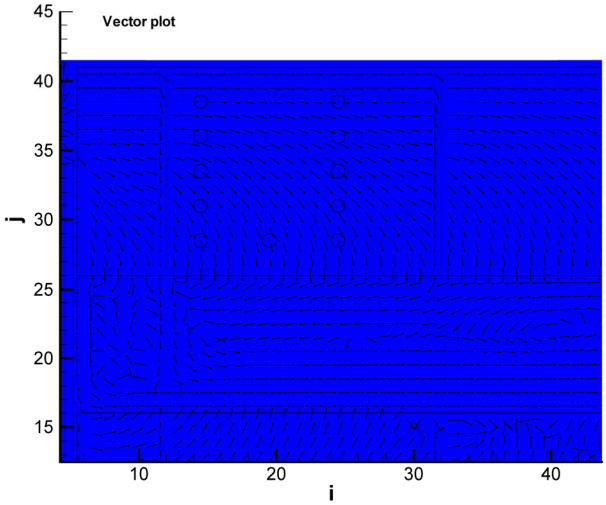

Figure 16. Uniform vector plot showing direction of water flow in the model.

actually starts to move in the opposite direction once it reaches the channel—this is caused by velocities in the channel—the higher permeability of the joint upstream of cross-section A causes water to exit the foam at a higher velocity here than the rest of the foam, causing the velocities in the channel to circulate, as shown in **Figures 16** and **17**. This explains the misleading shape of the plume in the models when it reaches the channel. It can be seen in the computer animations that the plume does actually move downstream after reaching the part of the channel with larger velocities.

For the Nov 2 B run, tracer was injected into hole A3. Tracer was observed to exit the foam after 11 minutes. The model predicts the plume to emerge at the same time but slightly closer to the injection hole as was observed. An animation of the model run shows that the main "slug" of tracer is predicted to emerge almost exactly at the observed point, but at a slightly later time than observed 15 min after injection, or 0.6 hours after the model start, since the injection occurs at 0.35 hours.

In run Nov 9 A, which involved injecting tracer into hole A5, the tracer was observed to emerge after 62 min. The model predicts that the tracer will emerge at the same time at a position slightly upstream, however, the joint

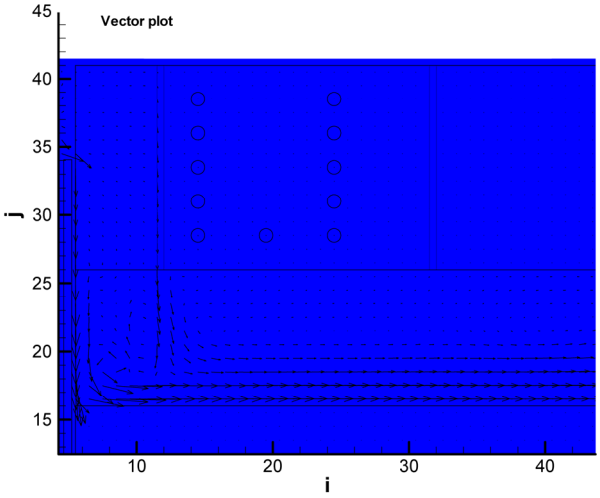

Figure 17. Relative vector plot showing direction and magnitude of water flow in the model.

between the foam blocks influences the tracer distribution significantly. Above was described how the model was adjusted to simulate the joints between the foam blocks by increasing the permeability and using open cells. This causes the tracer to move much faster along the joints in the model, and so the model predicts that the exit of the tracer will occur at two places. However, visible tracer was only observed at one exit point, and this was upstream of the joint between the foam blocks, in between the two exit points predicted in the model.

Two recordings of exit positions and time were made on run Nov 9 B. Tracer was injected into A5 and observed to exit at 56 minutes later at the point. After 79 minutes the position had moved to a point 9 cm further downstream, giving an average velocity of approx. 0.000065 m/s in the downstream direction for the point where the tracer plume exits the foam.

The model predicts an initial exit of the tracer nearly 50 cm upstream at the same time as the observed exit point, and by the second reading the main tracer plume exit point is still upstream of the observed point, although the joint causes tracer to leak into the channel closer to the observed point.

Three exit timings were recorded on run Nov 10. Injected into hole A5, the tracer was observed to exit at 57 minutes after the injection at a similar point to the previous runs. After 91 minutes, the exit point had moved downstream by 14 cm, then after 101 minutes it had moved a further 10 cm giving downstream velocities of 0.000069 m/s, and 0.000167 m/s, or an average of 0.000118 m/s.

The model again predicts an exit point upstream of the observed position but at the correct time, and the subsequent observations show the same pattern.

Comparing the observed apparent velocity of the edge of the tracer plume where it exits the foam with the modelled velocities shows a good correlation, as shown in **Figure 18**.

The two runs of Jan 29 and Jan 31 have identical parameters (injection duration, upstream and channel water level). Tracer injected at A5 appeared after 54 minutes at the same point each time (2.75 m on the flume ruler). The model again predicts that the tracer emerges at this time but further upstream (40 cm upstream approx.), however, the main slug of tracer reaches the channel at the observed point, but at a later time than observed.

The Feb 5 run is a similar scenario to Jan 29 and Jan 31, but with a slightly higher head elevation at the pumped end. Tracer injected into hole A5 emerged at 54 minutes at an identical location to the Jan 29 and Jan 31 runs, as shown in **Table 8**. This time the model predicts that the initial emergence of the tracer will be earlier than observed, due to the higher head difference between the upstream reservoir and the channel. By the time the tracer was observed to exit, the model predicts that a considerable amount of tracer will have already emerged into the channel. The bulk of the tracer did exit near the observed point, but at a later time (approx 63 min after injection or 9 minutes after it was observed).

For the Feb 7 run, tracer injected into hole A5 emerged 52.5 minutes later at the same location as the previous three runs. The model again predicts an earlier initial exit time and an exit point higher upstream, but significant bulk of the tracer exits at the observed point at a later time, as in the previous run.

5.2. Fluorometer Data

Using the same experimental set-up described above all the holes in cross-section C were monitored with fluorometers in order to measure the tracer concentration passing through each hole. However, out of all the experiments, only two peaks of tracer concentration were detected, both in hole C5—one in the Jan 12 run, and one in the Jan 31 run. These measured peaks are compared to the modelled concentrations for the Jan 12 run in **Figure 19**. The fluorometers did not detect any tracer on the low sensitivity

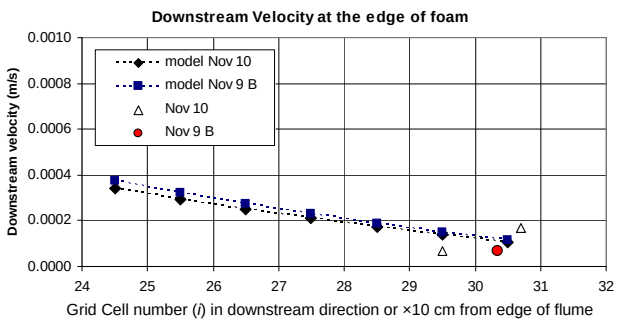

Figure 18. Downstream velocity at edge of the foam, measured and modelled.

setting, so in both cases the medium sensitivity setting was used, meaning that concentrations over 1000 ppb (0.001 ppt) were not measured. This meant that the peak concentration was not recorded, but the timing of the peak was still valid. The fluorometers were placed in the channel for the Feb 5 run and both fluorometers detected peaks in this run. The measured concentrations are plotted against the modelled concentrations for the same point in the channel in **Figure 20**.

5.3. Discussion of Tracer Experiments

It was hoped to measure peaks of tracer concentration in several different holes, but despite repeated experiments and endless calibration and repair, only one hole yielded a measurable peak. However, the tracer still exited the foam at the expected place or relatively close to the expected place. There could be a few reasons for this anomaly:

a) The tracer may not enter the monitoring hole at all but move round the holes if there is any resistance to flow into the hole itself. In cutting the hole perhaps the foam pores on the edge of the hole were made more resistant to flow, or perhaps the glue used to affix the plug into the base of the hole blocked up some of the foam pores, making a preferential flowpath around the monitoring hole. However, this is thought unlikely as tracer was observed in at least one of the monitoring holes;

b) The tracer could be travelling through the foam plug at the base of the monitoring hole and so be undetected by the fluorometer tube that takes a sample from the free water in the hole. This is unlikely because the glue used to secure the plug would, if anything, restrict flow through this plug;

c) the tracer could be bypassing the monitoring hole by short-circuiting underneath the foam or along the side of the blocks, although this is again unlikely due to the glue at the base of the foam securing it to the floor of the flume;

d) the tracer may not be evenly distributed over the depth of the water column. The fluorometer sampling tube necessarily only samples from one part of the water column and could miss the tracer if it moves in a "layer".

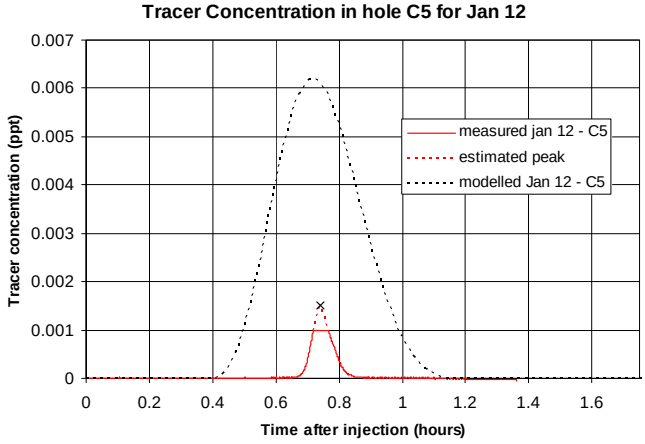

Figure 19. Tracer concentration in hole C5 for Jan 12.

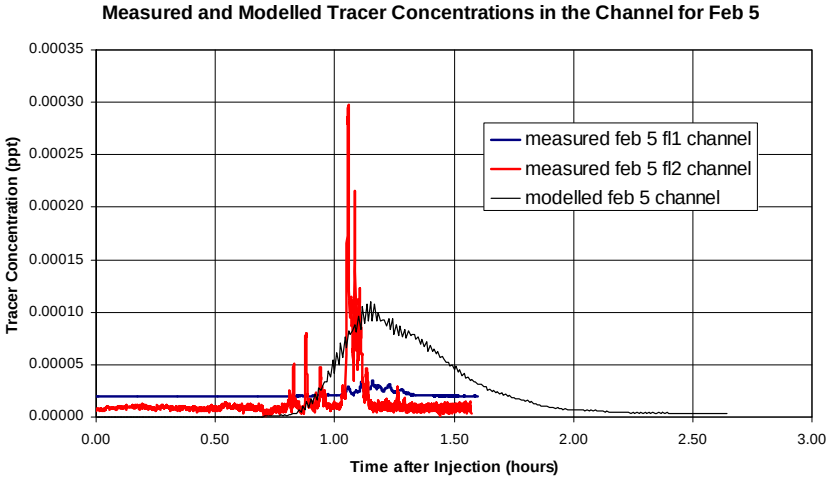

Figure 20. Tracer concentration in the channel (2.5 m on ruler) for Feb 5.

This possibility is perhaps reinforced by the observation that when the tracer emerges from the foam into the channel it appears at the top of the water column.

It is thought that of the suggested explanations, option d) is the most likely with perhaps option a) contributing slightly. Measurements were taken as near the surface of the water column as possible after this was decided, but the necessity of ensuring the fluorometer tube was always submerged limited the proximity to the water surface that could be achieved and no new tracer was detected in any of the holes.

The results that were obtained from hole C5 show good agreement with the modelled data. The timing of the modelled and observed peaks coincided almost exactly on the Jan 12 run, both occurring at approximately 43 mins after injection, although the modelled magnitude was considerably higher (at 0.0062 ppt) than the measured magnitude (estimated at 0.0015 ppt). The Jan 31 run appears to show a much larger measured peak, of the order of 0.0035 ppt at approximately 22 min after injection, much closer to the modelled peak of 0.0046 ppt, which occurs 3 min later.

The Jan 31 peak occurs sooner after injection than the Jan 12 peak, indicating that the tracer moved faster through the foam. This is borne out by the head difference recorded in Table 8. The run on Jan 12 had an upstream head of 18.0 cm, and a channel head of 8.1 cm, giving a 9.9 cm head difference. Jan 31 had a head of 24.0 cm upstream and 8.0 cm in the channel, giving a head difference of 16 cm, and hence faster velocities through the foam. The model predicts the same behaviour.

When the fluorometers were placed in the channel to catch the exit plume of tracer, the two fluorometers were placed side by side. Both recorded tracer peaks of different magnitudes, indicating the difficulty of exact measurement. Both were calibrated to the same scale and were responding accurately, yet fluorometer 1 records much lower concentrations than fluorometer 2. It can be seen in **Figure 20** that the tracer in the exit plume is not evenly mixed and that small eddies and disturbances cause the concentration to fluctuate at any given point, giving rise to the varied readings on the fluorometers in the channel, particularly as one fluorometer will be slightly closer to the centre of the plume than the other. The average of both the fluorometers gives a better match on the magnitude of the peak, however the peak is still sharper than the modelled. The timing of the peaks is more significant than the peak concentrations measured due to the difficulties of measuring the tracer. The modelled peak for the same location at the exit point of the plume shows good agreement for the timing of the exit point.

5.4. Exit Point Data

Data from the observed exit point of the tracer was much more easily obtained and allowed a more extensive comparison between the modelled and observed results. The results are encouraging; with the model predicting a similar flow pattern to the laboratory experiments, at least in terms of where the tracer exits the foam. An injection into hole A3 (Nov 2 B) quickly exits the foam after 10 minutes or so, at a point just upstream of cross-section B, and the model predicts very similar behaviour. An identical injection into A5 takes much longer to emerge (so much so that the first few experiments were abandoned in error before it had emerged) and eventually exits just upstream of cross-section D after nearly an hour. The model also predicts this behaviour, and the observed movement of the exit point of the plume is closely matched by that of the model; the modelled velocities at the edge of the foam agree well with these observations (18).

6. Conclusions

This is believed to be the first attempt to simulate groundwater in the laboratory using permeable foam, explaining the number of the difficulties encountered. Nevertheless, useful data have been obtained from the laboratory experiments, allowing the validity of the numerical model to be assessed.

The tidal basin in the Hyder Hydraulics Laboratory at Cardiff University was modified to allow simulated interactions between surface water and groundwater. Permeable foam blocks were used to represent permeable aquifers adjacent to a river. The properties of the foam were measured using several simple laboratory techniques, and values were determined for hydraulic conductivity (permeability) and porosity, evaluated as 0.002 m/s and 75% respectively.

The initial experimental set-up used weights to prevent the foam blocks from floating, however this did not prevent short-circuiting of the tracer underneath the foam blocks and the results obtained from this initial set-up were more indicative of problems in the laboratory set-up. After analysing these results, a series of improvements were suggested and carried out in the laboratory. The new laboratory set-up was used to collect water level information for a range of scenarios. The DIVAST-SG model was set-up to model these scenarios and predict the water levels in the foam. Modification to the input file to include representations of the joints between the foam blocks allowed a good fit between the observed and modelled water levels. The lack of an unsaturated flow model in the numerical model could account for some of the differences between the model and the observed behaviour. Tracer experiments were then carried out using Rhodamine-WT dye as in the initial experiments. Using the DIVAST-SG model that most accurately modelled the water levels, the tracer experiments were also modelled.

Tracer proved difficult to measure in the foam boreholes for a variety of possible reasons, however the results that were obtained agreed well with the model. Encouraging correlation was observed between the observed exit point of the tracer from the foam, and the modelled exit point and time.

7. Acknowledgements

The work carried out in this paper was supported by NERC studentship NER/S/A/2003/11216.

REFERENCES

[1] H. H. J. Cooper and M. I. Rorabaugh, "Ground-Water Movements and Bank Storage Due to Flood Stages in Surface Streams," US Geological Survey, 1963.

[2] G. F. Pinder and S. P. Sauer, "Numerical Simulation of Flood Wave Modification Due to Bank Storage Effects," *Water Resources Research*, Vol. 7, No. 1, 1971, pp. 63-70. doi:10.1029/WR007i001p00063

[3] R. E. Smith and D. A. Woolhiser, "Overland Flow on an Infiltrating Surface," *Water Resources Research*, Vol. 7, No. 4, 1971, pp. 899-913. doi:10.1029/WR007i004p00899

[4] R. Freeze and J. A. Cherry, "Groundwater," Prentice-Hall, Inc., Upper Saddle River, 1979.

[5] M. G. McDonald and A. W. Harbaugh, "A Modular Three-Dimensional Finite Difference Ground-Water Flow Model," US Geological Survey, 1988.

[6] H. E. Jobson and A. W. Harbaugh, "Modifications to the Diffusion Analogy Surface-Water Flow Model (DAFLOW) for Coupling to the Modular Finite-Difference Ground-Water Flow Model (MODFLOW)," US Geological Survey, Reston, 1999.

[7] M. L. Merrit and L. F. Konikow, "Documentation of a Computer Program to Simulate Lake-Aquifer Interaction Using the MODFLOW Ground-Water Flow Model and the MOC3D Solute-Transport Model," US Geological Survey, Tallahassee, 2000.

[8] J. I. Restrepo, A. M. Montoya and J. Obeysekera, "A Wetland Simulation Module for the MODFLOW Ground Water Model," *Ground Water*, Vol. 36, No. 5, 1998, pp. 764-770. doi:10.1111/j.1745-6584.1998.tb02193.x

[9] S. Panday and P. S. Huyakorn, "A Fully Coupled Physically-Based Spatially-Distributed Model for Evaluating Surface/Subsurface Flow," *Advances in Water Resources*, Vol. 27, 2004, pp. 361-382. doi:10.1016/j.advwatres.2004.02.016

[10] R. A. Falconer, "An Introduction to Nearly Horizontal Flows," In: M. B. Abbott and W. A. Price, Eds., *Coastal, Estuarial and Harbour Engineers' Reference Book*, E. & F. N. Spoon Ltd., London, 1993, pp. 27-36.

[11] R. A. Falconer, B. Lin, Y. Wu and E. Harris, "DIVAST Reference Manual," Hydro-Environmental Research Centre, Cardiff University, Cardiff, 2001.

[12] R. A. Falconer, B. Lin, Y. Wu and E. Harris, "DIVAST User Manual," Hydro-Environmental Research Centre, Cardiff University, Cardiff, 2001.

[13] T. Sparks, D. Kountcheva, B. Bockelmann and R. Falconer, "Physical and Numerical Modelling of Groundwater and Surface-Water Interactions with a Conservative Tracer," *ISSMGE Proceedings of 5th International Congress on Environmental Geotechnics*, Cardiff, June 2006.

[14] J. Baer, "Dynamics of Fluids in Porous Media," American Elsevier Publishing Company Inc., New York, 1972.

[15] H. Darcy, "Les Fontaines Publiques de la Ville de Dijon," Dalmont, Paris, 1856.

[16] K. Spanoudaki, A. Nanou, A. I. Stamou, G. Christodoulou, T. Sparks, B. Bockelmann and R. A. Falconer, "Integrated Surface Water-Groundwater Modelling," *Global Network of Environmental Science and Technology* (*NEST*) *Journal*, Vol. 7, No. 3, 2005.

[17] EC, "Directive 2000/60/EC of the European Parliament and of the Council of 23 October 2000 Establishing a Framework for Community Action in the Field of Water Policy," European Parliament and Council 2000/60/EC, 2000.

[18] BS1377, "Determination of Permeability by the Constant-Head Method," British Standards, Part 5, 1990.

[19] J. Dupuit, "Études Théoriques et Pratiques sur le Mouvement des eaux," Dunos, Paris, 1863.

[20] H. Rouse, "Engineering Hydraulics," John Wiley & Sons, Inc., Hoboken, 1950.

[21] Turner_Designs, "Application Support Bulletin 103: Fluorescein and a Fluorometer," 2006. http://www.turnerdesigns.com/t2/doc/appnotes/998_5103.html

